MIMO Free-Space Optical Communication Employing Subcarrier Intensity Modulation in Atmospheric Turbulence Channels

Zabih Ghassemlooy[1], Wasiu O. Popoola[1], Vahid Ahmadi[2], and Erich Leitgeb[3]

[1] Northumbria Communication Research Lab (NCRLab), Northumbria University, Newcastle upon Tyne, UK
fary.ghassemlooy@unn.ac.uk
[2] Department of Electrical Engineering Tarbiat Modares University, Tehran, Iran
[3] Institute of Broadband Communications, TU, Graz, Austria

Abstract. In this paper, we analyse the error performance of transmitter/receiver array free-space optical (FSO) communication system employing binary phase shift keying (BPSK) subcarrier intensity modulation (SIM) in clear but turbulent atmospheric channel. Subcarrier modulation is employed to eliminate the need for adaptive threshold detector. Direct detection is employed at the receiver and each subcarrier is subsequently demodulated coherently. The effect of irradiance fading is mitigated with an array of lasers and photodetectors. The received signals are linearly combined using the optimal maximum ratio combining (MRC), the equal gain combining (EGC) and the selection combining (SelC). The bit error rate (BER) equations are derived considering additive white Gaussian noise and log normal intensity fluctuations. This work is part of the EU COST actions and EU projects.

Keywords: Atmospheric turbulence, BPSK, Free-space optics, Laser communications, MIMO systems, Subcarrier modulation, Spatial diversity.

1 Introduction

Propagating data-laden laser radiation over the atmosphere termed FSO communications is attractive for a number of reasons including unlicensed spectrum and a narrow beamwidth [1-3]. There exist a global growing interest in FSO and it was extensively researched as part of the concluded EU framework 6 projects and the COST actions. Towards the end of 2008 a new COST action called IC0802 on "Propagation tools and data for integrated Telecommunication, Navigation and Earth Observation systems" was started and within this action group; our working group (consisting of around 10 participants) is involved in the optical wireless communications.

An outdoor FSO link is essentially based on line-of sight (LOS), thus, its spatial isolation from potential interferers is sufficiently maintained by its narrow beamwidth profile. But an obvious demerit of the narrow laser beamwidth is the pointing and tracking requirements in the event of misalignment. This can however be corrected using active tracking but at the cost of increased complexity and cost [3-5].

R. Mehmood et al. (Eds.): EuropeComm 2009, LNICST 16, pp. 61–73, 2009.

Fog, aerosols, rain and gases and other particles suspended in the atmosphere result in laser irradiance/intensity attenuation. The attenuation coefficient typically ranges from a few dB/km in a clear atmosphere to ~270 dB/km in a dense fog regime [4]. The huge attenuation suffered during dense fog restricts the carrier class FSO links to ~500 m [5, 6]; extending the link range in such conditions requires alternative schemes such as hybrid RF/FSO [7, 8]. Another factor that accounts for the FSO performance degradation in a clear atmosphere is the irradiance fluctuation (scintillation) and the phase fluctuation, which result from random index of refraction variations along the propagation path due to the atmospheric turbulence [3, 9, 10].

The On-Off keying (OOK) signalling format has been widely used in the commercially available FSO systems. But in channels with the atmospheric turbulence induced fading, the OOK scheme requires adaptive threshold to perform optimally [11, 12]. This fact among others has led to the increased interest in the study of SIM in FSO systems [12-14]. It has also been shown that using a fixed threshold OOK scheme results in suboptimal system, which is not only inferior to a SIM modulated FSO link but also has a BER floor [15]. In [16] the low density parity check (LDPC) coding has been explored to ameliorate the effect of scintillation on a SIM-FSO link. It is reported that the LDPC coded SIM in atmospheric turbulence achieved a coding gain of > 20 dB compared to the similarly coded OOK. In [17] the use of space-time block code with coherent and differential detection techniques has been reported to achieve a similar performance. However, invoking error control coding introduces huge processing delays and efficiency degradation in view of the number of redundant bits that will be required as outlined in [18].

In this paper the BER analysis of the SIM-FSO based multiple-input-multiple-output (MIMO) configuration in the presence of the log normal atmospheric turbulence is presented considering the following linear receiver combining techniques: EGC, MRC and SelC. Both cases of spatially correlated and uncorrelated optical field at the receivers are considered in the presence of the additive white Gaussian noise. In a related work reported in [19], the spatial diversity is considered at the receiver side for both OOK and PPM modulated FSO systems. Apart from mitigating scintillation, the MIMO system is advantageous in combating temporary link blockage by birds and misalignment when combined with a wide laser beamwidth, thereby eliminating the need for an active tracking. It also is much easier to provide independent aperture averaging with multiple separate aperture system. The terrestrial FSO is basically a LOS link with a negligible delay spread; hence inter-symbol interference (ISI) is not an issue. The rest of the paper is arranged as follows: Section 2 discusses subcarrier intensity modulation; the error performance is discussed in Section 3 while the concluding remarks are given in Section 4.

2 Subcarrier Intensity Modulation

In optical communication systems SIM is achieved by modulating the data onto a radio frequency signal, which is then used to vary the irradiance/intensity of an optical source (a continuous laser source in this case). In this work, the subcarrier is assumed to be pre-modulated using the BPSK. Other modulation methods can also be used and this is one of the major advantages of SIM. Considering weak turbulence and assuming that the log intensity l of laser radiation traversing the atmosphere

obeys the normal distribution i.e. $l \sim N(-\sigma_l^2/2, \sigma_l^2)$, then the probability density function (pdf) of the intensity $I = I_o \exp(l)$ is given by [20]:

$$p_I(I) = \frac{1}{\sqrt{2\pi}\sigma_l}\frac{1}{I}\exp\left\{-\frac{\left(\ln(I/I_0)+0.5\sigma_l^2\right)^2}{2\sigma_l^2}\right\} \quad I \geq 0, \tag{1}$$

where the average received intensity $I = 0.5I_{\max}$, I_{max} is the peak received laser intensity and I_0 is the received average intensity without turbulence. The σ_l^2 is a measure of the strength of laser intensity fluctuation and (1) is valid for $\sigma_l^2 < 1.2$ [20]. The instantaneous photocurrent can be modelled as [21]:

$$i_r(t) = RI(1+\xi m(t)) + n(t), \tag{2}$$

where ζ is the modulation index, R is the PIN photodetector responsivity and $n(t)$ is the additive white Gaussian noise (AWGN). Considering M subcarriers, the composite subcarrier signal during the kth symbol duration is given by:

$$m(t) = \sum_{j=1}^{M} A_j g(t - kT) d_k \cos(w_{cj} t + \varphi_j), \tag{3}$$

where $d_k \in \{-1,1\}$ for data bit '0' and '1', $g(t - kT)$ is the rectangular pulse shaping function, and T is the symbol duration. The subcarrier angular frequency and the phase are represented by $\{\omega_{cj}\}_{j=1}^{M}$ and $\{\varphi_{cj}\}_{j=1}^{M}$, respectively, while $\{A_j\}_{j=1}^{M}$ is the peak subcarrier amplitude. For the continuous wave laser transmitter to operate within its dynamic range and to avoid signal distortion due to clipping, the condition $|\zeta m(t)| \leq 1$ must always hold. Considering BPSK modulated subcarriers with non-varying amplitudes, the peak amplitude $A_j = A$. And if ζ is normalized to unity, then $A \leq 1/M$ During the kth symbol, the photocurrent is as given by:

$$i_r(t) = RI\left[1+\xi A\sum_{j=1}^{M} g(t-kT)d_k \cos(w_{cj}t+\varphi_j)\right] + n(t). \tag{4}$$

The band pass filters (BPF) in Fig.1 help separate the subcarriers and suppress any slow varying RI component in (4). The subcarrier frequencies are subsequently demodulated independently by frequency down conversion using a reference carrier signal $\cos(\omega_{cj}t + \varphi_j)$. A low pass filter (LPF) is employed to recover d_k with minimal distortion. The result per branch is an antipodal signal given by:

$$i_D(t) = \frac{d_k IR\xi A g(t-kT)}{2} + n_D(t), \tag{5}$$

where $n_D(t)$ is the post demodulation AWGN with a variance $\sigma^2/2$. The post demodulation electrical signal-to-noise ratio (SNR_e) γ, per subcarrier is then derived from (5) as:

$$\gamma(I) = \frac{(I\xi RA)^2}{2\sigma^2}. \tag{6}$$

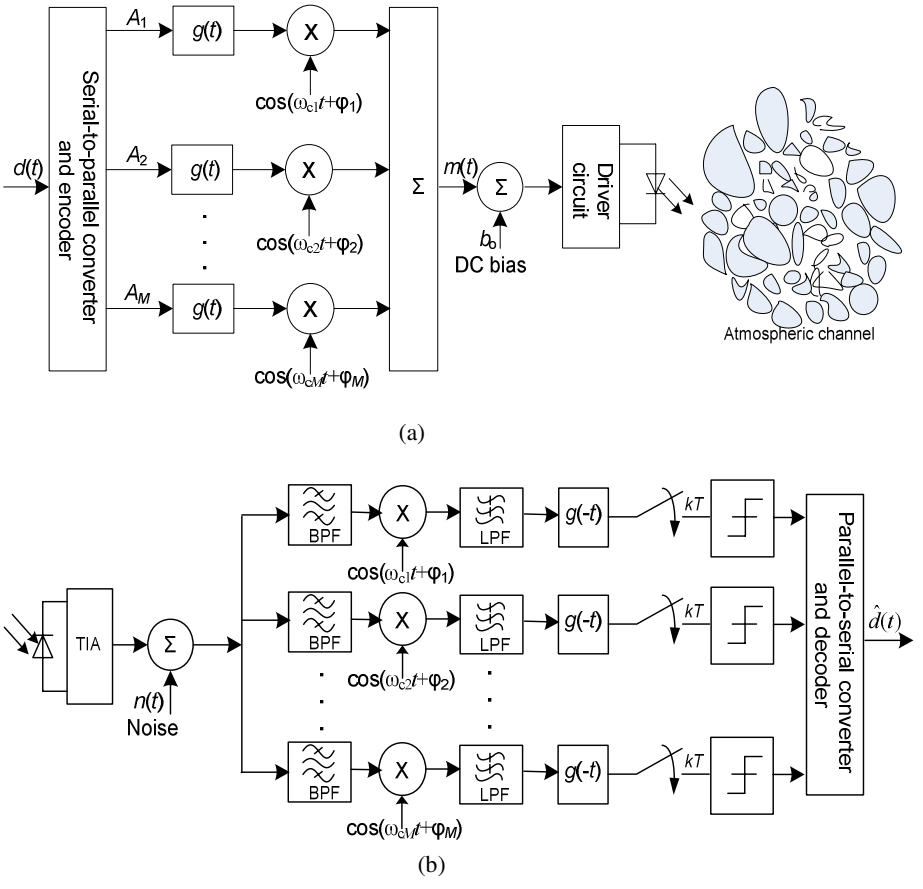

Fig. 1. SIM-FSO block diagram; (a) transmitter, and (b) receiver. TIA – Trans-impedance amplifier.

For a fixed value of ζ therefore, using multiple subcarrier increases throughput/capacity but at SNR_e penalty given by $20\log M$ dB. This suggests that multiple subcarriers should only be considered when the need for increased capacity outweighs the accompanying power penalty.

3 Error Performance

3.1 Without Diversity

For a coherently demodulated BPSK SIM operated in a channel with the atmospheric turbulence, the unconditional probability of bit error obtained by averaging the conditional error rate over irradiance fluctuation statistics is derived as [22]:

$$P_e \cong \frac{1}{\pi}\int_0^{\pi/2}\frac{1}{\sqrt{\pi}}\sum_{i=1}^{m} w_i \exp\left(-\frac{K^2\exp(2(\sqrt{2}\sigma_l x_i - {\sigma_l}^2/2))}{2\sin^2(\theta)}\right)d\theta$$
$$\cong \frac{1}{\sqrt{\pi}}\sum_{i=1}^{m} w_i\, Q(Ke^{(x_i\sqrt{2}\sigma_l - {\sigma_l}^2/2)}), \tag{7}$$

where $K = \frac{R\xi I_0 A}{\sqrt{2}\sigma}$, $\{x_i\}_{j=1}^{m}$ and $\{w_i\}_{j=1}^{m}$ represent the zeros of the mth order Hermite polynomial $He_m(x)$ and the corresponding weight factors, respectively.

3.2 With Receiver Diversity

Spatial diversity is employed both at the transmitter and receiver as shown in Fig. 2. In the analysis and the subsequent sections, the single SIM-FSO is considered. First, the use of an array of N-photodetector is analysed while transmitter array is treated in the subsequent section.

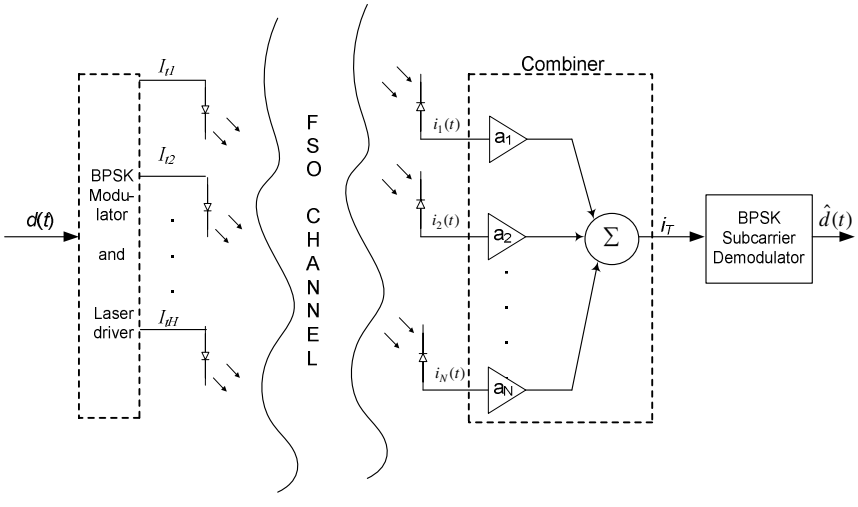

Fig. 2. $H \times N$-MIMO FSO system block diagram

We assume the spatial separation s of the photodetectors to be greater than the irradiance spatial coherence distance ρ_o (i.e. $s > \rho_o$) resulting in uncorrelated received irradiance. This assumption is realistic because ρ_o is on the order of few centimetre [20]. We also assumed that the beamwidth at the receiver is sufficiently broad to cover the entire field of view (FOV) of the N detectors. The photocurrents $\{i_{ri}(t)\}_{i=1}^{N}$ are linearly combined before being applied to the coherent demodulator to extract the transmitted data from the received subcarrier signal.

To facilitate a fair comparison between the single-transmitter-single-receiver system and the spatial diversity system, each aperture area in the photodetector array is assumed to be A_D/N, where A_D is the receiver aperture area for single-transmitter-single-receiver system. The SNR_e can thus be derived as:

$$\gamma = \frac{\left(RA\xi/2N\right)^2\left(\sum_{i=1}^{N} a_i I_i\right)^2}{\sum_{i=1}^{N} a_i^2 \sigma_i^2/2N} \le \frac{\left(RA\xi/2N\right)^2 \sum_{i=1}^{N} a_i^2 \sum_{i=1}^{N} I_i^2}{\sum_{i=1}^{N} a_i^2 \sigma_i^2/2N}. \tag{8}$$

MRC

Under the MRC, the gains $\{a_i\}_{i=1}^{N} \equiv \{I_i\}_{i=1}^{N}$ resulting in the optimum SNR_e given below:

$$\begin{aligned} \gamma_{MRC}(\vec{I}) &= \left(\frac{RA\,\xi}{\sqrt{2N}}\right)^2 \sum_{i=1}^{N} \frac{I_i^2}{\sigma_i^2} \\ &= \sum_{i=1}^{N} \gamma_i, \end{aligned} \tag{9}$$

where $\gamma_i = \left(\frac{RA\xi I_i}{\sqrt{2N\sigma_i^2}}\right)^2$ is the *SNR* for each link. The unconditional BER with the MRC linear combining is given by [22]:

$$\begin{aligned} P_{e(MRC)} &= \int_0^{\infty} Q\left(\sqrt{\gamma_{MRC}(\vec{I})}\right) P_{\vec{I}}(\vec{I})\, d\vec{I} \\ &= \frac{1}{\pi}\int_0^{\pi/2} \left[S(\theta)\right]^N d\theta \end{aligned}, \tag{10}$$

Where $S(\theta) \approx \frac{1}{\sqrt{\pi}} \sum_{J=1}^{M} w_j \exp\left(-\frac{K_o^2}{2\sin^2\theta} \exp\left[2\left(x_j\sqrt{2}\sigma_l - \sigma_l^2/2\right)\right]\right)$ and $K_o = \frac{R\xi I_o A}{\sqrt{2N}\sigma}$. Next, we consider the sub-optimum but more practical linear combining techniques.

EGC

For the EGC, gains $\{a_i\}_{i=1}^{N}$ in (8) are all made constant, thus resulting in the following SNR_e:

$$\gamma_{EGC}(\vec{I}) = \left(\frac{RA\,\xi}{\sqrt{2N}\sigma}\right)^2 \left(\sum_{i=1}^{N} I_i\right)^2 < \left(\frac{RA\,\xi}{\sqrt{2N}}\right)^2 \sum_{i=1}^{N} \frac{I_i^2}{\sigma^2}. \tag{11}$$

Thus, $\gamma_{EGC}(\vec{I}) < \gamma_{MRC}(\vec{I})$ and the unconditional BER can be obtained as [22]:

$$P_{e(EGC)} = \int_0^{\infty} \frac{1}{\pi} \int_0^{\pi/2} \exp\left(-\frac{K_1^{\,2}}{2\sin^2(\theta)} Z^2\right) P_Z(Z)\, d\theta dZ = \frac{1}{\sqrt{\pi}} \sum_{i=1}^{m} w_i\, Q(K_1 e^{(x_i\sqrt{2}\sigma_u + \mu_u)}) \quad (12)$$

where $K_1 = \frac{R\xi I_0 A}{\sqrt{2}\,\sigma N}$, $P_z(Z) = \frac{1}{\sqrt{2\pi}\sigma_u} \frac{1}{Z} \exp\left\{-\left(\ln Z - \mu_u\right)^2 / 2\sigma_u^{\,2}\right\}$ and

$\mu_u = \ln(N) - \frac{1}{2}\ln\left(1 + \frac{e^{\sigma_l^2} - 1}{N}\right)$ while $\sigma_u^{\,2} = \ln\left(1 + \frac{e^{\sigma_l^2} - 1}{N}\right)$.

SelC

Here, the combiner samples all $\{i_{ri}(t)\}_{i=1}^{N}$ and selects the link with the highest SNR_e, its BER is derived as [22]:

$$P_{e(SelC)} = \frac{2^{1-N} N}{\sqrt{\pi}} \sum_{i=1}^{m} w_i \left[1 + erf(x_i)\right]^{N-1} Q(K_0 \exp(x_i\sqrt{2}\sigma_l - \sigma_l^{\,2}/2)), \quad (13)$$

3.3 Effect of Signal Correlation on the BER

For *N*-photodetector separated by a spatial distance less than the laser radiation spatial coherence distance (i.e. $s < \rho_0$), the received radiations are correlated. To show the effect of this on the system error performance, we consider *N* equally spaced photodetectors employing the optimum MRC linear combining. The unconditional BER in atmospheric turbulence is obtained by averaging (14) over the joint pdf of the intensity fluctuations.

$$P_{ec} = Q\left(\sqrt{\gamma_{MRC}(\vec{I})}\right) = \frac{1}{\pi} \int_0^{\pi/2} \exp\left(-\frac{K_0^{\,2}}{2I_0^{\,2}\sin^2\theta} \sum_{i=1}^{N} I_i^{\,2}\right) d\theta \quad (14)$$

Adopting the Tatarski approach [20], the correlation coefficient $\rho(s) = B_X(s)/B_X(0)$ of an optical wave in turbulent atmosphere between two points with a spatial separation *s* is given by:

$$\rho(s) = 1 - 2.36(ks/L)^{5/6} + 1.71(ks/L) - 0.024(ks/L)^2 + 0.00043(ks/L)^4 + \ldots \quad (15)$$

where $k = 2\pi/\lambda$; it can be inferred that the correlation coefficient is inversely proportional to the spatial separation s for $\frac{s}{\sqrt{\lambda L}} < 1$ (i.e. for s less than atmospheric channel coherence distance) from which the covariance matrix (16) is obtained.

$$C_X = \begin{bmatrix} \sigma_x^2 & \rho\sigma_x^2 & . & . & \rho\frac{s_{12}}{s_{1N}}\sigma_x^2 \\ \rho\frac{s_{12}}{s_{21}}\sigma_x^2 & \sigma_x^2 & . & . & . \\ . & . & . & . & . \\ . & . & . & . & . \\ \rho\frac{s_{12}}{s_{N1}}\sigma_x^2 & . & . & . & \sigma_x^2 \end{bmatrix}, \tag{16}$$

where s_{ij} is the spatial separation between photodetectors i and j, $\sigma_x^2 = \sigma_l^2/4$ is the log amplitude variance while ρ is the correlation coefficient between two photodetectors with spatial separation s_{12}. The joint pdf of received laser intensity is given by [9]:

$$p_{\vec{I}}(\vec{I}) = \frac{1}{2^N \prod_{i=1}^{N} I_i} \frac{1}{(2\pi)^{N/2}\left|C_X\right|^{1/2}} \exp(-\frac{1}{8}\beta C_X^{-1}\beta^T), \tag{17}$$

where $\beta = \left[\ln\frac{I_1}{I_0} \quad \ln\frac{I_2}{I_0} \quad . \quad . \quad . \quad \ln\frac{I_N}{I_0} \right]$. The expression for the unconditional BER is then obtained as:

$$P_e = \int_0^\infty p_{\vec{I}}(\vec{I}) Q(\sqrt{\gamma_{MRC}(\vec{I})}) d\vec{I}\,. \tag{18}$$

3.4 Transmitter Diversity

In this case we consider a single photodetector and multiple laser transmitters. The laser sources are assumed to be sufficiently spaced so that the photodetector receives uncorrelated laser radiations. To ensure a fair comparison and to maintain a constant power requirement, we assume that the power available for a single-transmitter system is equally shared amongst the H-laser transmitters. As such, the irradiance from each laser represents an H factor reduction compared to a single transmitter system. Another obvious approach is to assume that all the transmitters have the same power; in this case the power requirement will have to increase by a factor H [18]. Based on the former, the received photocurrent is given by:

$$i_r(t) = \sum_{i=1}^{H} \frac{R}{H} I_i \left(1 + A\xi d_k g(t - kT)\cos(w_c t + \varphi)\right) + n(t)\,. \tag{19}$$

Since laser arrays are only separated by a few centimetres, the phase shift experienced by the received irradiance due to path difference is therefore negligible. The SNR_e on each subcarrier can therefore be derived as:

$$\gamma_{MISO}(\vec{I}) = \left(\frac{R\xi A}{\sqrt{2}H\sigma}\right)^2 \left(\sum_{i=1}^{H} I_i\right)^2. \tag{20}$$

There exist a clear similarity between (11) and (20) hence; the unconditional BER for the multiple transmitter-single photodetector system is the same as that for the single transmitter-multiple photodetector configuration with EGC linear combining.

3.5 Transmitter Diversity-Receiver Diversity (MIMO)

In this section we consider a multiple-laser and multiple-photodetector system. In consistent with the earlier assumptions, the total transmit power is made equal to the transmit power when using a single laser to achieve the same bit rate and the combined aperture area of the *N*-photodetector is the same as when a single photodetector is used. The *H*-laser and *N*-photodetector are assumed spaced enough so that the received laser radiations are uncorrelated. First, we consider when the photocurrents are combined using EGC. As previously discussed, a multiple transmitter-single photodetector system with *H*-laser is identical to a single transmitter-multiple photodetector configuration having *H*-photodetector with EGC combining; thus the following represents the SNR_e assuming identically distributed irradiance:

$$\gamma(\vec{I}) = \left(\frac{R\xi A}{\sqrt{2}NH\sigma}\right)^2 \left(\sum_{i=1}^{N}\sum_{j=1}^{H} I_{ij}\right)^2 = \left(\frac{R\xi A}{\sqrt{2}NH\sigma}\right)^2 \left(\sum_{i=1}^{NH} I_i\right)^2. \tag{21}$$

This expression is the same as *NH*-photodetector single transmitter-multiple photodetector system employing EGC linear combining. Hence, the unconditional BER is obtained by replacing *N* by *NH* in (12).

By linearly combining the photocurrents using MRC, the individual SNR_e on each link is:

$$\gamma_i(I_i) = \left(\frac{R\xi A}{\sqrt{2N\sigma^2 H}} \sum_{j=1}^{H} I_{ij}\right)^2. \tag{22}$$

Considering the sum of independent lognormal distributed random variables as another log normal distribution [23] then the unconditional BER is derived as:

$$P_e = \frac{1}{\pi}\int_0^{\pi/2} \left[S(\theta)\right]^N d\theta, \tag{23}$$

Where $S(\theta) \approx \frac{1}{\sqrt{\pi}}\sum_{J=1}^{M} w_j \exp\left(-\frac{K_2^2}{2\sin^2\theta}\exp\left[2\left(x_j\sqrt{2}\sigma_u + \mu_u\right)\right]\right)$, $K_2 = \frac{R\xi I_O A}{\sqrt{2N}\sigma H}$, σ_u^2 and μ_u are as previously defined except that *N* is now replaced by *H*. For an optical MIMO-FSO link under consideration therefore, the BER performance is governed by (12) with *N* replaced by *NH* for the EGC combining technique and (23) for the MRC.

3.6 Results and Discussions

The plot of (7) against the normalised electrical *SNR* $(RE[I]/2\sigma)^2$ is shown in Fig. 3 with $M = [1, 2, 5, 10]$, $\sigma_l^2 = 0.3$ and $\zeta = 1$. When $M = 1$ the BER curve is the same as that reported in [12]. Multiple subcarriers can therefore be used to increase the capacity but at an electrical SNR penalty defined by $20\log M$ dB. To show the effect of signal correlation, (18) is plotted in Fig. 4 for $N = [2, 3]$ and $\rho = [0, 0.1, 0.3, 0.6]$ at a turbulence level $\sigma_l^2 = 0.3$. To achieve a BER of 10^{-6}, the use of two photodetectors with $\rho = 0.3$ and 0.6 require additional ~1.8 dB and ~3.5 dB of *SNR*, respectively, compared to when $s > \rho_o$ (i.e. when $\rho = 0$); with three photodetectors, the additional *SNR* required to achieve the same BER of 10^{-6} is ~2.7 dB and ~5 dB for $\rho = 0.3$ and 0.6, respectively. This apparently shows the effect of correlated intensity and also buttresses the emphasis placed on the need for s to be greater than ρ_o in a spatial diversity system as it results in the maximum gain.

To compare the MIMO system with the single SIM benchmark reported in [12], the BER given by (23) is plotted against the normalised electrical *SNR* as depicted in Fig. 5 at a turbulence level $\sigma_l^2 = 0.3$ for various values of N and H. The link margin (diversity gain) resulting from the use of transmitter/receiver array is shown in Table I. A 2 × 2-MIMO system requires an additional ~0.4 dB of *SNR* compared to a 1 × 4-MIMO system. In the latter however, 4 photodetectors will have to be sufficiently spaced to avoid any correlation in the received signals as against 2 photodetectors in the former. Also, at the stated BER, a 4 × 4-MIMO based SIM-FSO link requires ~4 dB and 1 dB lower *SNR* compared to the single transmitter with 4 and 8 photodetectors, respectively.

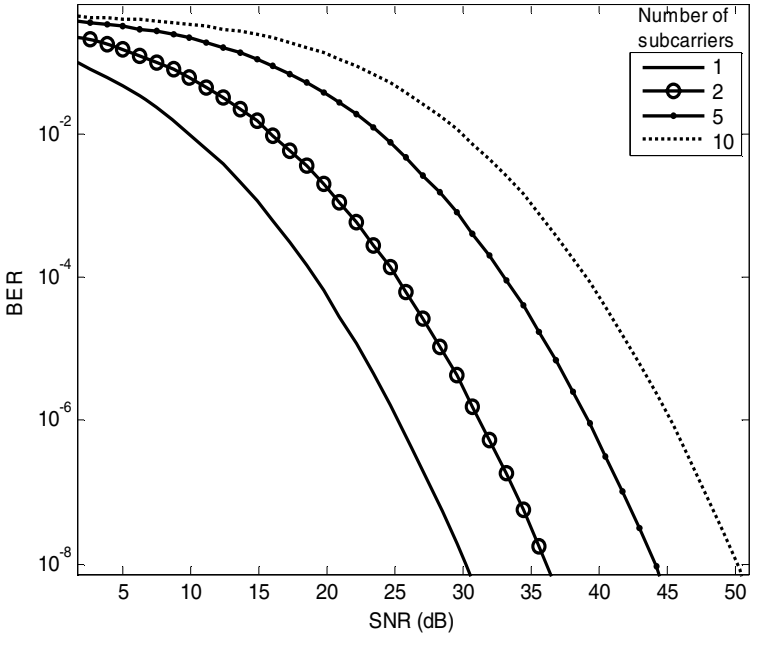

Fig. 3. BER against the electrical *SNR* for $M = [1,2,5,10]$ subcarriers and turbulence strength $\sigma_l^2 = 0.3$

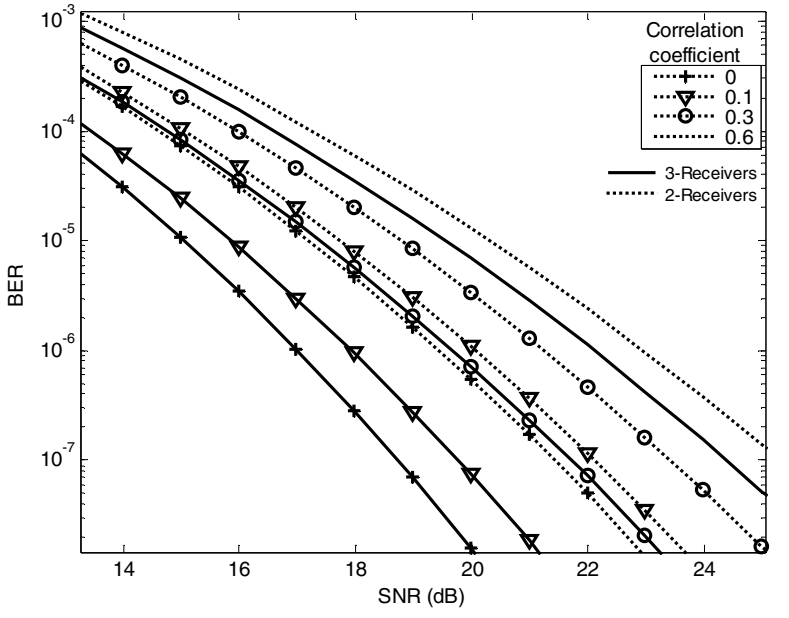

Fig. 4. BER against the electrical *SNR* at different values of correlation coefficient for number of photodetector $N = [2, 3]$ and turbulence strength $\sigma_I^2 = 0.3$

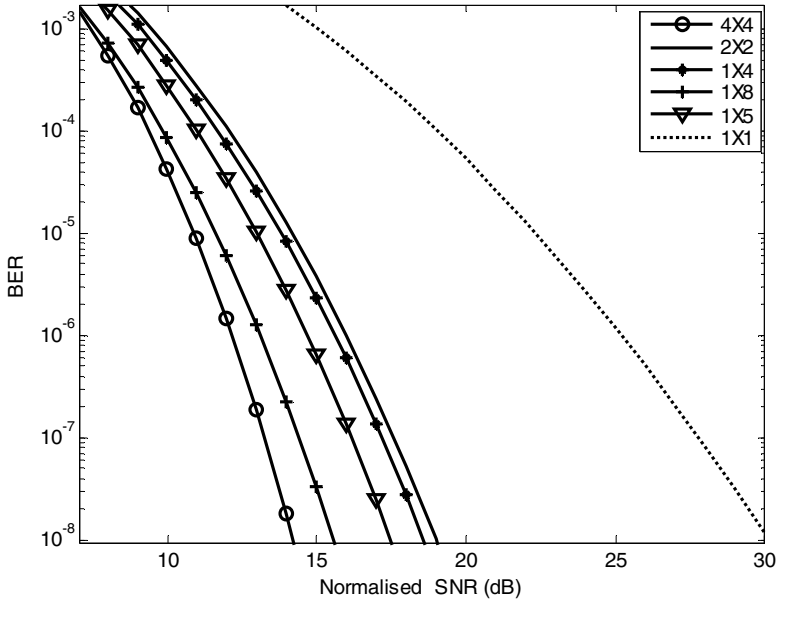

Fig. 5. MIMO BER against the electrical *SNR* for different numbers of laser and photodetector array at turbulence strength $\sigma_I^2 = 0.3$ and $M = 1$

Table 1. Link margin (diversity gain) at BER of 10^{-6} and $\sigma_l^2 = 0.3$

MIMO configuration	1x5	1x8	4x4	2x2	1x4
Link margin (dB)	10.5	12.1	13.1	9.2	9.6

4 Conclusions

We have presented an expression for the unconditional BER of *H*×*N*-MIMO FSO system that uses BPSK subcarrier intensity modulation under the log normal distributed weak atmospheric turbulence environment. The error performance and the link margin (theoretical) using three different linear combining techniques have also been presented. Results showing clearly the effect of correlated received irradiance on the system error performance have also been given. In a 2-detector array and at a turbulence strength σ_l^2 of 0.3, a correlation coefficient of 0.6 results in additional ~3.5 dB of SNR to achieve a BER of 10^{-6}; this incurred power penalty increases as the received signals become more correlated. At a BER of 10^{-6}, 2 × 2-MIMO systems require ~0.4 dB additional *SNR* when compared with 1 × 4-MIMO systems. But spacing of an array of 4 photodetectors to ensure uncorrelated irradiance reception is far more demanding than spacing 2 photodetectors. Also the use of 4 × 4-MIMO to deliver the same BER of 10^{-6} requires ~4 dB and 1 dB lower SNR than using one laser source with 4 and 8 photodetectors, respectively. A 4 × 4-MIMO system is thus the preferred configuration to mitigate scintillation without increased system complexity.

References

1. Uysal, M., Jing, L., Meng, Y.: Error rate performance analysis of coded free-space optical links over gamma-gamma atmospheric turbulence channels. IEEE Transactions on Wireless Communications 5, 1229–1233 (2006)
2. Leitgeb, E., Geghart, M., Birnbacher, U.: Optical networks, last mile access and applications. Journal of optical and fibre communications reports 2, 56–85 (2005)
3. Kedar, D., Arnon, S.: Urban Optical Wireless Communication Networks: The main challenges and possible solutions. IEEE Optical communications, s2–s7 (2004)
4. Willebrand, H., Ghuman, B.S.: Free Space Optics: Enabling optical Connectivity in today's network. SAMS publishing, Indianapolis (2002)
5. Killinger, D.: Free space optics for laser communication through the air. Optics & Photonics News, 36–42 (October 2002)
6. Kim, I.I., McArthur, B., Korevaar, E.: Comparison of laser beam propagation at 785 nm and 1550 nm in fog and haze for optical wireless communications. In: SPIE Proceeding: Optical Wireless Communications III, vol. 4214, pp. 26–37 (2001)
7. Bloom, S., Hartley, W.S.: The last-mile solution: hybrid FSO radio, in AirFiber, Inc. White paper (Visited, July 2007), `http://www.freespaceoptic.com/WhitePapers/Hybrid_FSO.pdf`
8. Kim, I.I., Korevaar, E.: Availability of free space optics and hybrid FSO/RF systems. In: Proceedings of SPIE: Optical wireless communications IV, vol. 4530, pp. 84–95 (2001)
9. Zhu, X., Kahn, J.M.: Free-space optical communication through atmospheric turbulence channels. IEEE Transactions on Communications 50, 1293–1300 (2002)

10. Karp, S., Gagliardi, R.M., Moran, S.E., Stotts, L.B.: Optical Channels: fibers, cluds, water and the atmosphere. Plenum Press, New York (1988)
11. Huang, W., Takayanagi, J., Sakanaka, T., Nakagawa, M.: Atmospheric optical communication system using subcarrier PSK modulation. In: ICC 1993, IEEE International Conference on Communications, Geneva, May 1993, vol. 3, pp. 1597–1601 (1993)
12. Ohtsuki, T.: Turbo-coded atmospheric optical communication systems. In: IEEE International Conference on Communications (ICC), New York, pp. 2938–2942 (2002)
13. Kim, J.P., Lee, K.Y., Kim, J.H., Kim, Y.K.: A performance analysis of wireless optical communication with convolutional code in turbulent atmosphere. In: International Technical Conference on Circuits Systems, Computers and Communications (ITC-CSCC 1997), Okinawa, pp. 15–18 (1997)
14. Popoola, W.O., Ghassemlooy, Z., Leitgeb, E.: Free-space optical communication using subcarrier modulation in gamma-gamma atmospheric turbulence. In: 9th International Conference on Transparent Optical Networks (ICTON 2007), Rome, Italy, vol. 3, pp. 156–160 (2007)
15. Li, J., Liu, J.Q., Taylor, D.P.: Optical communication using subcarrier PSK intensity modulation through atmospheric turbulence channels. IEEE Transaction on communications 55, 1598–1606 (2007)
16. Djordjevic, I.B., Vasic, B., Neifeld, M.A.: LDPC coded OFDM over the atmospheric turbulence channel. Optical Express 15, 6336–6350 (2007)
17. Yamamoto, H., Ohtsuki, T.: Atmospheric optical subcarrier modulation systems using space-time block code. In: IEEE Global Telecommunications Conference (GLOBECOM 2003), New York, vol. 6, pp. 3326–3330 (2003)
18. Lee, E.J., Chan, V.W.S.: Optical communications over the clear turbulent atmospheric channel using diversity. IEEE Journal on Selected Areas in Communications 22, 1896–1906 (2004)
19. Razavi, M., Shapiro, J.H.: Wireless optical communications via diversity reception and optical preamplification. IEEE Transaction on Communications 4, 975–983 (2005)
20. Osche, G.R.: Optical Detection Theory for Laser Applications. Wiley, New Jersey (2002)
21. Gagliardi, R.M., Karp, S.: Optical Communications, 2nd edn. John Wiley, New York (1995)
22. Popoola, W.O., Ghassemlooy, Z., Allen, J.I.H., Leitgeb, E., Gao, S.: Free-space optical communication employing subcarrier modulation and spatial diversity in atmospheric turbulence channel. IET Optoelectronic 2, 16–23 (2008)
23. Mitchell, R.L.: Permanence of the log-normal distribution. Journal of the optical society of America 58, 1267–1272 (1968)